International Journal of Biological Macromolecules 149 (2020) 672–681

Contents lists available at ScienceDirect

International Journal of Biological Macromolecules

journal homepage: http://www.elsevier.com/locate/ijbiomac

Encapsulation of phycocyanin by prebiotics and polysaccharides-based electrospun fibers and improved colon cancer prevention effects

Yan Wen [a,1], Peng Wen [a,1], Teng-Gen Hu [a,b], Robert J. Linhardt [c], Min-Hua Zong [a], Hong Wu [a,*], Zhi-Yi Chen [b,*]

[a] School of Food Science and Engineering, South China University of Technology, Guangdong Province Key Laboratory for Green Processing of Natural Products and Product Safety, Guangzhou 510640, China

[b] Sericultural & Agri-Food Research Institute, Guangdong Academy of Agricultural Sciences, Key Laboratory of Functional Foods, Ministry of Agriculture, Guangdong Key Laboratory of Agricultural Products Processing, Guangzhou 510610, China

[c] Department of Chemical and Biological Engineering, Center for Biotechnology and Interdisciplinary Studies, Rensselaer Polytechnic Institute, Troy, NY 12180, USA

ARTICLE INFO

Article history:
Received 16 June 2019
Received in revised form 9 October 2019
Accepted 20 January 2020
Available online 22 January 2020

Keywords:
Coaxial electrospinning
Phycocyanin
Prebiotics
Cancer prevention
Cell cycle arrest
Apoptosis

ABSTRACT

To preserve bioactivity and achieve colon targeted release of phycocyanin (PC), the polysaccharides-based electrospun fiber mat (EFM) containing PC and prebiotics was prepared and characterized. In vitro release tests confirmed the colon targeting behavior of PC, in particular, faster release of PC was achieved due to the addition of prebiotics. Ritger–Peppas model confirmed that the release of PC in simulated colon fluids follows a mechanism of anomalous transport (non-Fickian). CCK-8 results showed that the combination of PC and prebiotics exerted a significant anti-proliferative effect on HCT116 cells with an IC50 values of 22.31, 17.12 and 11.63 mg/mL after 24, 48, and 72 h, respectively. Furthermore, the cell cycle and apoptosis analysis revealed that the inhibition activity on HCT116 cells was caused by arresting cell cycle at G0/G1 phase that is relevant to the inhibition of cyclin D1 and CDK4 and the up-regulation of p21 expression, and inducing cell apoptosis by mediating the mitochondrial pathway as well, in which the decrease of Bcl-2/Bax, activation of caspase 3 and release of cytochrome *c* were included. This study suggests that the PC-loaded EFM with GOS holds a great potential as an effective formulation for colon cancer prevention.

© 2020 Elsevier B.V. All rights reserved.

1. Introduction

Colon cancer is the leading cause of cancer-related death. Although much effort has been applied to conventional therapies (like surgery, intravenous, and radiation therapy) for treating colon cancer, poor patient compliance and numerous side effects (including nausea, vomiting and bloody stools, etc.) are associated with conventional therapy. Colon targeted drug delivery is regarded as an attractive option as it possesses high specificity, improved efficacy and reduced adverse effects [1]. A good approach for achieving colonic delivery involves the utilization of carriers that can be degraded under the action of colonic microflora [2]. Polysaccharides have gained much attention in developing such microflora-activated colon specific release systems, and many of polysaccharides-based systems for colon-targeted delivery have been reported [3,4]. Recently, prebiotics that are indigestible in the upper gastro intestinal tract (GIT) are also becoming preferred substrates for construction of colonic-targeted delivery, furthermore, the efficacy of prebiotics for the stimulation of microflora and the role in the treatment of colon carcinogenesis have been demonstrated [5,6]. Hence, using polysaccharides and prebiotics (such as galacto-oligosaccharide, GOS) for colonic delivery holds promise.

Bioactive compounds have received special attention as anti-cancer agents within the functional food and nutritional industries. Phycocyanin (PC), a water-soluble biliprotein, is of great interest as it exhibits considerable in vitro and in vivo anticancer activity on a variety of cancer cell types [7]. In addition, administration of even high doses (from 0.25 to 5.0 g/kg body weight) of PC does not induce noticeable symptoms of toxicity nor mortality in animals [8], suggesting the therapeutic potential of PC in cancer treatment. Unfortunately, PC exhibits poor stability and is sensitive to the harsh environment of upper GIT, and thus the envisioned benefits are severely compromised. Encapsulation and targeted delivery of PC to the colon is desiderated to preserve its activity, enhance its bioavailability and enable localized treatment for colon cancer.

Abbreviations: PC, Phycocyanin; EFM, electrospun fiber mat; IBD, inflammatory bowel disease; GIT, gastro intestinal tract; GOS, galacto-oligosaccharide; DS, diclofenac sodium; PVP, polyvinylpyrrolidone; SCFAs, short chain fatty acids; CS, Chitosan; PEO, polyoxyethylene; PVA, polyvinyl alcohol; TPP, tripolyphosphate; PI, Propidium iodide; DAPI, dihydrochloride fluoropure grade; FTIR, Fourier transform infrared spectroscopy; TEM, transmission electronmicroscope; SEM, scanning electron microscopy; SGF, simulated gastric fluid; SIF, simulated intestinal fluid; SCF, simulated colon fluid; SDS–PAGE, sodium dodecyl sulfate–polyacrylamide gels; SD, standard deviation; Vc, Vitamin C; CDKs, cyclin-dependent kinases; CDKIs, CDK inhibitors.

* Corresponding authors.
E-mail addresses: bbhwu@scut.edu.cn (H. Wu), chenzhiyi@gdaas.cn (Z.-Y. Chen).

[1] The authors have the same contribution and are co-first authors.

https://doi.org/10.1016/j.ijbiomac.2020.01.189
0141-8130/© 2020 Elsevier B.V. All rights reserved.

Recently, nanotechnology has emerged as an efficient and promising approach for targeted delivery of bioactive agents. Nano-encapsulation based techniques have attracted tremendous attention for preserving the activity of bioactive compounds against adverse conditions and for enhancing the therapeutic efficacy [9]. So far, various kinds of nano - structured delivery systems, such as solid lipid nanoparticles, nano-hydrogel, nano-liposomes, nanoparticles, nano-fiber and micelles have been constructed [10,11], among which, nano-fiber is emerging as the leading nano-encapsulation carriers in developing delivery systems. Compared to other techniques (e.g., island-in-sea, self-assembly, phase separation, etc.), electrospinning is generally regarded as the preferred technique for generating nano-fibers from natural biopolymers as it provides design flexibility and high encapsulation efficiency [12–14]. The versatility of electrospinning is further enhanced by using coaxial electrospinning [15]/electrospraying [16], which can be exploited to create solid core-sheath structured fibers or core-shell nanoparticles, functional nanocoating [17,18] and monolithic nanofibers[19]/particles[20] as well. Thus, they can provide a series of strategies for encapsulating and protecting the fragile functional compounds [21]. In addition, different dissolution and targeted release behavior for compounds can be achieved by selecting the suitable core/shell materials [22,23]. For example, Rostami et al. developed resveratrol loaded chitosan-gellan nanofiber as a novel gastrointestinal delivery system, and the results revealed that the nanofibers have almost the same cytotoxicity against HT29 cancer cells compared to free resveratrol [24]. In another study, the core-shell structural nanocomposite for the colon-specific pulsatile release of diclofenac sodium (DS) was successfully prepared by modified coaxial electrospinning using polyvinylpyrrolidone (PVP)–DS as core and shellac as shell [25]. Moreover, multi-compartment systems for the controlled release of bioactive compounds have been prepared through coaxial electrospinning. Li et al. [26] reported that the particular two-stage drug release behavior of naproxen (NAP) could be achieved by embedding NAP-loaded liposomes in the core matrix of core-sheath nanofibers made with a sodium hyaluronate core and a cellulose acetate sheath. In this study, burst release of NAP was obtained for the first 8 h followed by a sustained release behavior lasting for 12 days. Hence, electrospinning is now being intensively studied in the food packaging, functional foods and pharmaceutical fields [27,28].

In our recent study, the incorporation of PC and hydrophobic molecule quercetin by polysaccharide-based electrospun fibers was achieved and its colon-specific performance was demonstrated [29,30]. However, the feasibility of using prebiotics and polysaccharides for colon-specific delivery of PC has not been investigated. There is a very limited understanding of the benefits of PC-loaded electrospun fiber mat (PC-loaded EFM) with GOS, such as its stimulation effect on probiotics, its enhanced anti-cancer activity, and the possible mechanism of apoptosis induced by short chain fatty acids (SCFAs, fermented from GOS) in combination with PC on cancer cells in vitro. This study involves the fabrication of a novel prebiotic and polysaccharide-based colon-specific delivery system for PC using coaxial electrospinning. The ability of this system to minimize PC release in the upper GIT and to undergo enzymatic hydrolysis in colon was investigated. The prebiotic activity on probiotics was assessed through evaluation of the bacterial population, pH changes and the production of SCFAs. The synergistic inhibition and underlying mechanism of action of PC-loaded EFM with GOS on the proliferation of HCT116 were also explored.

2. Materials and methods

2.1. Materials

PC with the purity ratio (A620/A280) of 2.04 was obtained from Taizhou Binmei Biotechnology Co., Ltd., Taizhou, China; GOS ($C_{30}H_{52}O_{26}$) was purchased from New Francisco Biotechnology Company (Guangdong, China); Chitosan (CS, DD was 87%) was purchased from Dacheng Biotech. Co. Ltd. (Weifang, China). β-Glucosidase, sodium alginate (SA, viscosity 15–25 cps), polyoxyethylene (PEO, 100 kDa), polyvinyl alcohol (PVA) and tripolyphosphate (TPP) were purchased from Sigma-Aldrich Company (Shanghai, China). Antibodies were obtained from Cell Signaling Technology (Danvers, MA, USA). Propidium iodide (PI), dihydrochloride fluoropure grade (DAPI) and annexin V-FITC/PI apoptosis detection kit were provided by Beyotime Biotechnology Co. Ltd. (Shanghai, China). *Bifidobacteria adolescentis (B. adolescentis) and Lactobacillus fermentum (L. fermentum)* were provided by Professor Hanju Sun (Hefei University of Technology).

2.2. Preparation and characterization of PC-loaded EFM with GOS

First, the PCNP was obtained according to the ionic-gelation method based on preliminary tests. TPP solution (1 mg/mL) was added into the CS (3 mg/mL, dissolved in 1% acetic acid, pH 5.3) solution that had been previously mixed with PC (1.5 mg/mL) solution to achieve the mass ratio of 5:1 for CS: TPP. The PCNP spontaneously formed and was collected by centrifugation at 18,000 rpm for 15 min at 10 °C. The interaction among the components was investigated by Fourier transform infrared spectroscopy (FTIR) spectrophotometer. Antioxidant activity of PCNP was investigated through its reducing power as previously described by Thangam et al. [31] with higher absorbance indicating the increased antioxidant capacity. OH• radical scavenging assay was performed following the method of Wang et al. [32]. The PC-loaded EFM was then prepared by co-axial electrospinning. The composition of the electrospinning solution was as follows: the core solution was composed of the PCNP and PVA (10% w/w) in a volume ratio of 2:1, and the SA and PEO (total polymer 9%, 80:20, w/w) in water ethanol (90:10, v/v) comprised the sheath polymer solution. For PC-loaded EFM with GOS, 3% (g/mL) of GOS was also added into the core solution. The sheath and core solutions were fed into a concentric spinneret at a sheath and core fluid flow rate of 0.12 and 0.29 mL/h, respectively. The core-sheath fibers were produced from a voltage of 17.2 kV and a distance of 15.6 cm. The morphology of obtained film was characterized by scanning electron microscopy (SEM, Carl Zeiss Jena, Germany). The core-sheath structure of the fibers obtained was investigated by transmission electron microscope (TEM, JEM-Z300FSC, JEOL, Japan) and confocal laser scanning microscopy (CLSM, LSM 510 META, Carl Zeiss Inc. USA) by labeling SA and CS with fluorescein isothiocyanate and rhodamine, respectively [33].

2.3. Evaluation of prebiotic activity of the PC-loaded EFM with GOS

The prebiotic activity of the PC-loaded EFM with GOS was evaluated by investigating its growth promotion effects on *B. bifidum* and *L. acidophilus*, respectively. The MRS basal media for the strains was prepared according to previously reported methods [34]. MRS without any carbon source was used as the negative control. Probiotics were cultured by adding 5 vol% bacterial suspension into culture solution and then placing in a CO_2 incubator at 37 °C for 48 h. Samples of the fermentation broths were withdrawn at different times, and the prebiotic activities of the films were evaluated by determining OD600, final pH values, and the content of short chain fatty acids (SCFAs). All experiments were carried out in duplicate.

2.4. In vitro release test

The release profile of PC from EFM containing GOS was examined in simulated gastric fluid (SGF, pH 1.2), simulated intestinal fluid (SIF, pH 6.8) and simulated colon fluid (SCF, pH 7.4) according to previously described methods [30]. A 5% of bacterial suspension was added in the SCF. At scheduled time internals, the PC content was measured for absorbance by using a UV–Vis spectrophotometer. Data was obtained at least in triplicate ($n = 3$), and was expressed as mean ± standard

deviation (SD). The Ritger–Peppas model was also employed to fit the release data of PC to investigate the release mechanism:

Ritger-Peppas: $\frac{M_t}{M_\infty} = kt^n$

(where M_t/M_∞ is the fractional PC release; k is a kinetic constant, and n is the diffusional exponent that corresponds to transport mechanism)

2.5. CCK-8 assay

CCK-8 assay was used to investigate the inhibitory effect of PC-loaded EFM with GOS on colon cancer HCT116 cells. Cells were cultured and treated as the previously described [30]. Various amounts of film were then immersed into the following fluids: SGF for 2 h, SIF for 4 h and SCF for 16 h to obtain the released PC medium. Subsequently, 100 μL of the released PC medium from SCF was added into a 96-well plate, while the same volume of fresh SCF medium was used as a control. After incubation for a specified time, the IC_{50} (inhibitory concentration resulting in 50% cell reduction) value was calculated. The inhibition effect of SCFAs was performed as follows: first, the digested PC-loaded EFM with GOS was fermented by *B. adolescentis* for 24 h, then 100 μL of fermented culture medium containing a range of concentrations of butyrate, propionate, acetate and lactic acid was added to the 96 well plates. Fermented culture medium (100 μL) was added to the 96-well plates. After incubating for 24, 48, and 72 h at 37 °C in 5% CO_2, cell viability by the SCFAs was also determined using CCK-8 assay. Thus, the effect of PC-loaded EFM with GOS could be obtained by calculating the inhibition rate of released PC medium and the SCFAs from the digested sample.

2.6. Cell cycle and apoptosis analysis

To investigate the effect of PC-loaded EFM with GOS on HCT116 cells cycle and apoptosis, firstly, 2×10^5 HCT116 was placed into the 24-well plates and cultured for 24 h. Then, the released PC medium and the fermented culture medium obtained as the steps described in Section 2.5 were added into the plate. After 24 h incubation, the cells were collected and washed twice with cold PBS for the cell cycle and apoptosis analysis. For cell cycle analysis, cells were first fixed gently with 80% ethanol at 4 °C for 2 h. Then, cells were centrifuged and treated with PI and RNase A in a dark room for 20 min, and the percentage of cell phase was analyzed using a flow cytometer (Becton Dickinson, Mountain View, CA, USA). Regarding apoptosis, the cells were centrifuged to remove supernatant followed by adding binding buffer to resuspend the cells. Thereafter, the annexin V-FITC and PI were added and the samples were kept in the dark for 20 min at 4 °C.

2.7. Western blot analysis

Cells were treated with the released PC medium and the fermented culture medium to detect the change in protein levels associated with apoptosis and cells cycle arrest. Cells were collected and washed with cold PBS. Proteins (30 μg/lane) were resolved on sodium dodecyl sulfate–polyacrylamide gels (SDS–PAGE), and then transferred to PVDF membranes. Afterwards, the blot was soaked in blocking buffer (Tris buffered saline (TBS, 20 mM)-Tween 20 (0.1%, v/v) solution with 5% non-fat milk) for 2 h, followed by incubation with individual monoclonal antibodies in blocking buffer at 4 °C overnight. Then, a secondary antibody horseradish peroxidase conjugate was added and detected by enhanced chemiluminescence reagents. The intensity of β-actin signals indicated the equal amounts of proteins and the gray-scale ratio of protein/β-actin were analyzed by Image J software.

2.8. Statistical analysis

Statistical analysis was performed by one-way analysis of variance (ANOVA). $P \leq 0.05$ means there is a significant difference in different groups.

3. Results and discussion

3.1. Characterization of PCNP and PC-loaded EFM with GOS

The morphology of the resulting PCNP and PC-loaded EFM with GOS are shown in Fig. 1a and b. As shown in TEM image, the PCNP was of a spherical shape with a particle size of around 50 nm. For fiber morphology, SEM image clearly indicates that the fibers were uniform and smooth and the TEM image verified the core–sheath structure of fibers obtained with the core being 220 nm and sheath layer being 370 nm in diameter. CLSM was further performed to provide a direct evidence. As shown in Fig. 1c, the image of fiber emitted both green and red fluorescence, which revealed that the core layer of CS labeled with RhB was indeed encapsulated into the sheath layer of SA labeled with FITC. As expected, a core–sheath structure was successfully constructed. The physical and chemical bonds involved in interaction in the encapsulation process were investigated by FTIR (Fig. 1d). It can be used to examine the entrapment of bioactive compounds into chitosan nanoparticle and the disappearance of characteristic peaks of encapsulated compounds indicates the interaction between the drug and the polymer [35]. In this study, PC exhibited a broadband between 3600 and 3000 cm^{-1}, which was related to O—H stretching and N—H stretching vibration. Moreover, the characteristic peaks of PC at 1666 cm^{-1}, 1535 cm^{-1} and 1455 cm^{-1} involving C═O stretching, N—H stretching and C—N stretching, respectively [36], have been diminished or disappeared suggesting a possible complexation between PC and chitosan. Previous studies have reported that drugs possessing an active hydrogen atom i.e. a hydrogen atom that has an extra electron in its outer shell that gives it a negative charge can be interacted with chitosan by hydrogen bonds or electrostatic interactions [37,38]. These findings are considered as a proof of the encapsulation of PC in the nanoparticle. Similarly, the disappearance of characteristic peaks of quercetin after encapsulation was also observed in chitosan nanoparticles by other studies [39]. Thus, we conclude that PC has been completely and successively encapsulated into the core of CS nanoparticles. Similar peaks for encapsulated PC were also reported by Chen et al. [40].

The stability of a protein is of great importance for its function and biological applications. Fig. 1(e) showed the UV–visible absorbance of PC under different pH conditions. We observed that the highest absorbance at 620 nm was recorded at pH 6 and 7, suggesting that the conformational structure was stable. However, the absorbance was slightly affected at pH 9.0, and the spectrum of the PC changed drastically at the acidic pH of 3.0. The decreased absorbance observed at pH 3.0 was attributed to the low solubility of PC around its isoelectric point, while the change in absorbance observed at the highly alkaline pH of 9.0, could be due to the electronic state of chromophore and direct affects on PC conformation. Since the encapsulation of PC into CS nanoparticle occurred at pH 5.3, we found that the spectrum of PC was nearly unchanged, indicating the stability of PC during the formation of PCNP. Then, the antioxidant activity of the encapsulated PC was investigated by reducing power and OH radical scavenging assays. Vitamin C (Vc) was used as positive control. As shown in Fig. 1f, there was a linear correlation between the absorbance and PC concentration. The IC_{50} value for scavenging OH· radicals was 592 μg/mL for PCNP, while the value was 537 μg/mL for free PC (data not shown). Thus, the results indicates that PC was effectively encapsulated into the CS nanoparticle.

3.2. Stimulation effects of PC-loaded EFM with GOS on the growth of probiotics

Since the promotion effects of prebiotics on probiotics have been demonstrated [41], two typical probiotics (*B. adolescentis* and *L. fermentum*) were applied to evaluate the prebiotic activity of the functional PC-loaded EFM with GOS. As depicted in Fig. 2a and b, an increase in OD_{600} and a decrease in pH value of the culture media were observed, indicating the promotion effect of PC-loaded EFM with GOS on

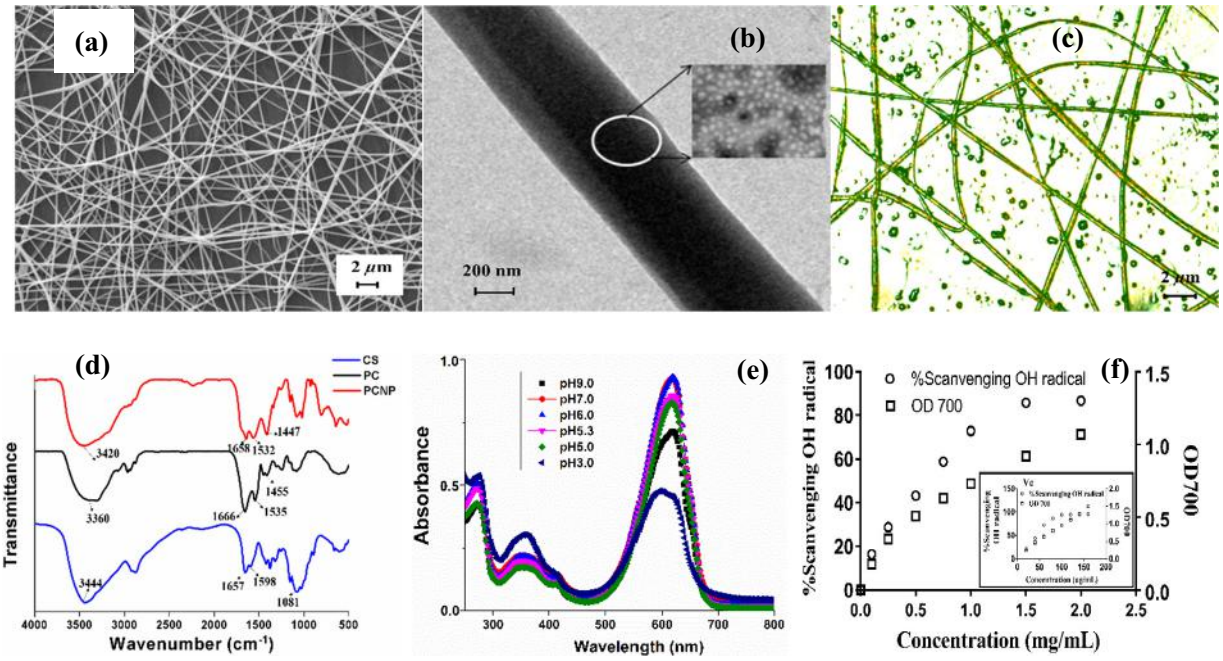

Fig. 1. (a) SEM image of PC-loaded EFM containing GOS; (b) TEM image of obtained fiber and PCNP; (c) CLSM image of obtained fiber (d)FTIR spectra of different sample; (e) absorption spectrum of PC under different pH; (f) antioxidant activity of different concentrations of PC-loaded EFM containing GOS.

probiotics. Since the decreased pH was caused by the fermentation of GOS, changes in the levels of organic acids were also studied and the results are shown in Fig. 2c and d. Generally, lactic acid is an intermediary product of during fermentation and can be converted into additional SCFAs by other intestinal bacteria [42]. The major SCFAs are acetic acid, propionic acid and butyric acid, which have important effects on colon function and health. Acetate is the most abundant part of the SCFAs and is primarily responsible for decreased pH. Propionic acid mainly serves as a precursor for gluconeogenesis and also has positive effect on the prevention of colon cancer. Butyric acid is also deemed to have a favorable impact on the growth and differentiation of colonic epithelial cells. However, butyrate is not a common end-product from the fermentation of *Lactobacilli* and *Bifidobacteria*, its production originates from the fermentation by other intestinal flora and a portion of the butyrate may be formed from acetate, as butyrate producing bacteria can utilize acetate [43]. Fig. 2c and d showed that the lactic acid and SCFAs

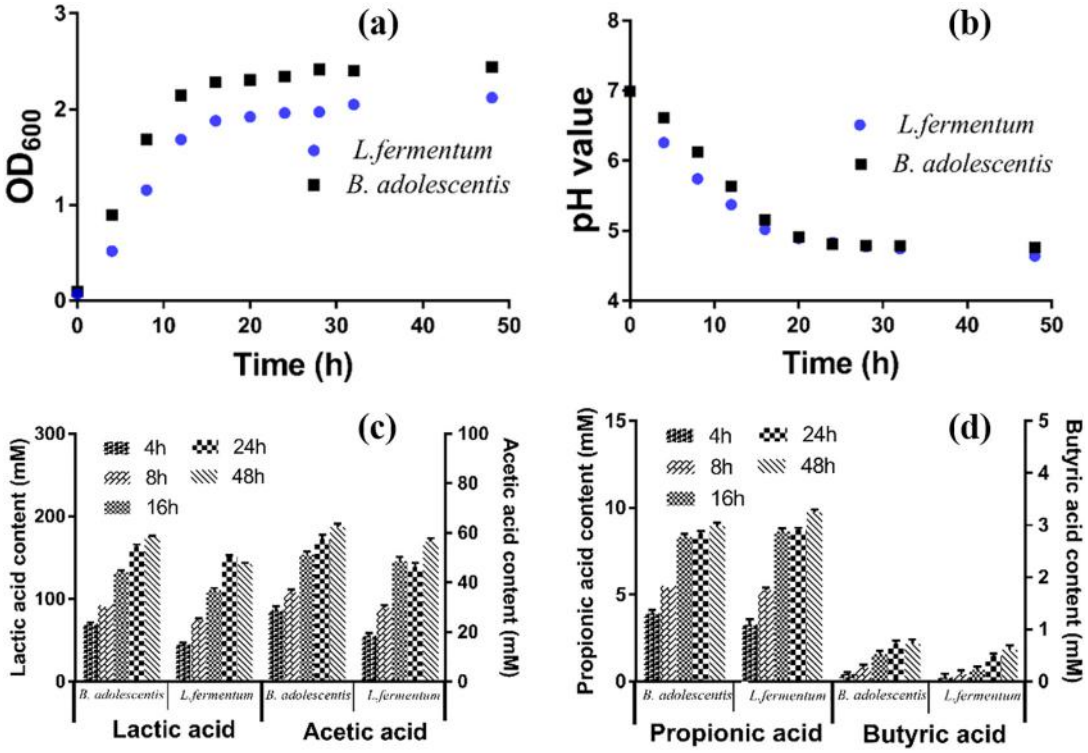

Fig. 2. Effect of different concentrations of PC-loaded EFM containing GOS on the growth curve (a) and final pH value (b) of *B. bifidum* and *L. acidophilus*; (c, d) the production of lactic acid and short chain fatty acids (mM) by *B. bifidum* and *L. acidophilus*.

concentration (especially for acetic acid) increased with incubation time for all films, and the concentration of lactic acid was higher than that of other organic acids. Acetate is the most abundant SCFA, followed by propionic acid and butyric acid. These results confirmed that probiotics were able to hydrolyze prebiotics-loaded EFM and to produce beneficial SCFAs.

3.3. In vitro release profile of PC

The release behavior of PC from PC-loaded EFM with GOS in different simulated fluids was also investigated. From Fig. 3a, about 15% of PC was released in SGF and SIF, while around 82% of PC could be released in SCF over 20 h. The release profile confirmed the colon-targeted behavior of PC. In particular, we discovered that a higher release rate of PC was obtained with the addition of prebiotics, as about 75% and 53% of PC were released after 12 h for PC-loaded EFM with or without GOS, respectively (Fig. 3b). This may be attributed to the production of organic acids by the fermentation of GOS, as depicted in Fig. 2, leading to the decreased pH that is also favorable for the dissolution of CS besides the degradation of CS carrier by β-glucosaccharase. These results indicate that the presence of prebiotics leads to the enhanced colon-specific targeting behavior.

Generally, the release mechanism could be classified as Fickian that is afforded by swelling or through relaxation (non-Fickian), which is related to anomalous transport. The mechanisms involved in release are important for predicting the in vivo release behavior of active compounds. Hence, the release kinetics were studied by fitting the release data with the Ritger–Peppas equation (at $M_t/M_\infty < 0.6$) to investigate the release mechanism of PC [44]. A value of $n \le 0.45$ means a Fickian diffusion mechanism. For the n value between 0.5 and 1, it corresponds to an anomalous transport or non-Fickian mechanism. In particular, the value of n equals to 1 indicating the kinetic is zero-order release [45]. In an ideal release model, it is desirable to have zero-order kinetics as this means the total release of the encapsulated compounds [46]. The release data (in SCF) fit well to the Ritger–Peppas equation (Fig. 3a, small figure). Compared to PC-loaded EFM, the higher n value (0.986 vs. 0.945) for PC-loaded EFM with GOS suggests the release of PC follows a mechanism of anomalous transport (non-Fickian), wherein its release is controlled by the polymer erosion [45].

The morphology of film after incubation in SGF, SIF and SCF over a given time was observed by SEM to investigate the stability of the electrospun fibers in aqueous environment (Fig. 3c–f). We can see that the film showed no obvious change and the surface remained smooth after 2 h in SGF (Fig. 3c and d). After the transferation of film

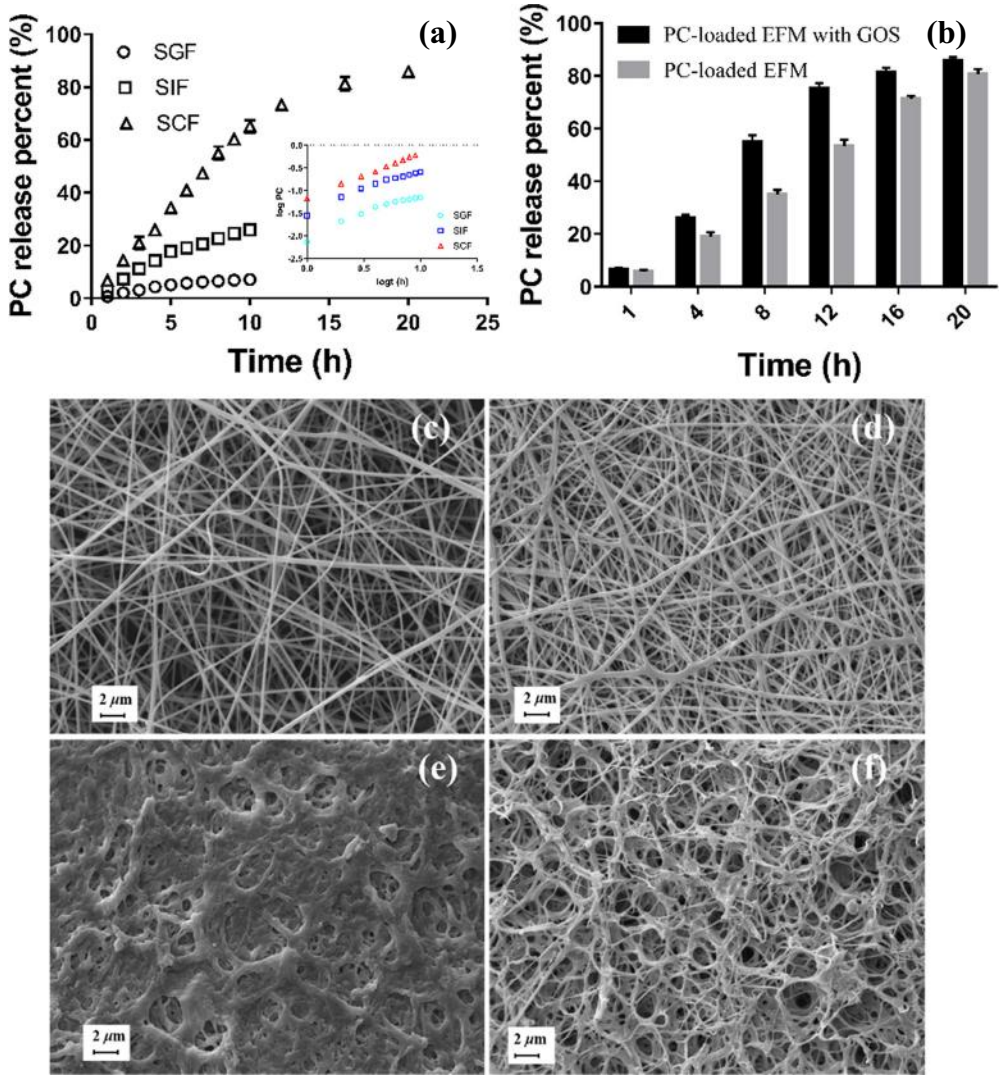

Fig. 3. (a) Release profile of PC from PC-loaded EFM containing GOS in different simulated digestive fluids, in which, the small figure was the Riger-peppas model of PC release data; (b) Release profile of PC from different film in SCF; (c-f) SEM images of PC-loaded EFM containing GOS: (c) and after exposure to the SGF for 2 h (d), SIF for 4 h (e), SCF for 10 h (f), respectively.

into SIF for the subsequent 4 h, the fibers gradually expand and their surface became rough (Fig. 3e). Finally, when the film was transferred into SCF, obvious changes were observed, as the fibers became thinner and more holes and cracks emerged (Fig. 3f). This was because at pH 1.2 (SGF), the protonation of SA in the sheath layer reduced the solubility of film, thus keeping the intact core-sheath structure. At higher pH (pH 6.8), the carboxyl groups of SA were deprotonated and ionized, favouring the solubilisation of sheath layer which would cause the swelling or collapse of film, despite that, the protonated amino groups ($-NH^{3+}$) on CS favoured a relative compact and stable core structure, which hindered the PC release from the core layer. However, in SCF, the CS core layer could be degraded by β-glucosidase or dissolved due to the decreased pH that caused by SCFAs, thus triggering PC release in SCF. The morphology change indicates that the obtained film showed resistance to the acid and digestive enzymes but was sensitive to be degraded in the colon, hence, is a promisting colon targeted delivery system.

3.4. Inhibition effect of PC-loaded EFM with GOS on HCT 116 cells

PC has been extensively investigated for its anti-cancer activity. SCFAs are the principal end products of prebiotic fermentation in the colonic lumen, which also exhibits beneficial functions on the inhibition of colon cancer cells. Dyer et al showed that butyrate was the most potent inhibitor of cell proliferation, followed by propionate and then acetate [47]. In this study, Fig. 2 showed that GOS can generates approximately 60 mM acetate, 9 mM propionate and 0.3 mM butyrate (Fig. 3). Hence, the growth inhibitory effect of PC-loaded EFM with GOS on HCT116 cells was determined using CCK-8 assay. From Fig. 4a, we can see that blank EFM without PC and GOS did not exhibit cytotoxic activity toward HCT116 cells, however, a significant decrease ($P < 0.05$) in cell proliferation was observed for PC-loaded EFM with GOS. The data also demonstrated that the combination of PC and GOS resulted in a greater inhibitory affects than treatment with PC or GOS alone on the growth of HCT116 cells. After 48 h, the cell viability treated by PC-loaded EFM alone, GOS alone and PC-loaded EFM with GOS were 68.7%, 81.5% and 58.9%, respectively. We can conclude that the combination of PC and GOS exerted a significant anti-proliferative effect on HCT116 cells when compared with PC or GOS alone ($P < 0.05$). This effect was in a dose- and time-dependent manner for PC-loaded EFM with GOS (Fig. 4b), as the IC_{50} values were 22.31, 17.12 and 11.63 mg/mL after 24, 48 and 72 h, respectively. The current study clearly indicates that the PC-loaded EFM with GOS exhibited enhanced inhibition effects on HCT116 cells.

3.5. Expression of proteins involved in regulation of cell cycle

Cell cycle regulation plays an important role in cell proliferation [48]. It had been reported that PC could induce G1 cell cycle arrest in colon cancer HT-29 cells and breast cancer MDA-MB-231 cells [49,50], as well as block G2/M cell cycle progression in pancreatic cancer PANC-1 cells [51]. SCFAs can also mediate the protective action by modulating the expression of genes involved in cell cycle arrest [52]. Thus, the distribution of HCT116 cell phase after exposure to PC-loaded EFM with GOS was examined. As shown in Fig. 5a, an accumulation of cells in the G0/G1 phase (from 52.9% in control to 60.6% and 68.9%) was observed, while a proportional reduction in the S and G2/M phase fractions were occurred after the GOS-alone and PC-alone treatment, respectively. These results revealed that PC-alone and GOS-alone individually induce G0/G1 phase arrest. When HCT116 cells were treated with PC-loaded EFM with GOS for 48 h, the proportion of G1 phase reached 74.8%, 14.4% of cells were found in S phase, and 10.8% in G2/M phase. Compared to other groups, there was a significant increase in the G0/G1 phase in PC-loaded EFM with GOS treated cells, indicating the synergistic effect of PC and GOS on cell cycle arrest in G0/G1 phase.

The levels of cell cycle regulatory genes involved in G0/G1 transition were tested to further confirm the above results. Cell cycle is controlled by a family of cyclin-dependent kinases (CDKs), which are regulated positively by its activating partner cyclins and negatively by CDK inhibitors (CDKIs), such as P21 [53]. The balance between CDK activation and inactivation determines whether cells proceed through G_1 into S phase and from G_2 to M phase. Among the cyclins, cyclin D1, the G0/G1 checkpoint regulator, is a rate limiting for cell cycle progression. Western blot analysis (Fig. 5b–d) revealed that PC-loaded EFM with GOS synergistically decreased the expression of cyclin D1 and its upstream kinase of CDK4 with a concomitant up-regulation of the cell cycle inhibitors P21 in a dose-dependent manner, supporting the observed G1 cell cycle arrest.

3.6. Apoptosis analysis and the expression of related proteins

It is known that the therapeutic effect of bioactive compounds is associated with cell cycle arrest, followed by initiation of apoptotic process. The apoptosis of HCT116 cells was analyzed by annexin-V/PI double staining assay. Representative results are shown in Fig. 6a and b. The control HCT116 cells were considered to be viable cells as they were negative for Annexin or PI staining. Nevertheless, apoptosis was induced in PC-loaded EFM with GOS treated cells, and the early and late apoptotic cell numbers were 60.7% and 10.0% vs. 0.1% and 0.0% in control, whereas the values were 21.8% and 3.9% for GOS only treated cells, and 47.2% and 7.3% for PC only treated cells, respectively. The

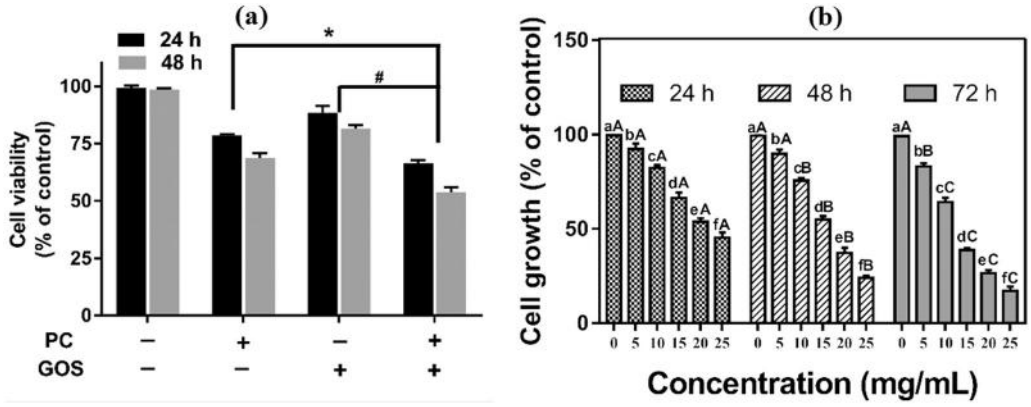

Fig. 4. (a) Combined effect of PC and GOS on HCT116 cell growth. $^{*}P < 0.0.05$ indicates statistically significant differences from the PC treatment group and $^{\#}P < 0.05$ indicates statistically significant differences from the GOS treatment group; (b) Effect of different concentrations of PC-loaded EFM containing GOS on HCT116 cells proliferation at different times. Analysis significance was determined. Concentrations within the same treatment time not sharing same lowercase letters are significantly different ($P < 0.05$). The different capital letter represents a significant difference ($P < 0.05$) among different incubation time at a specific concentration.

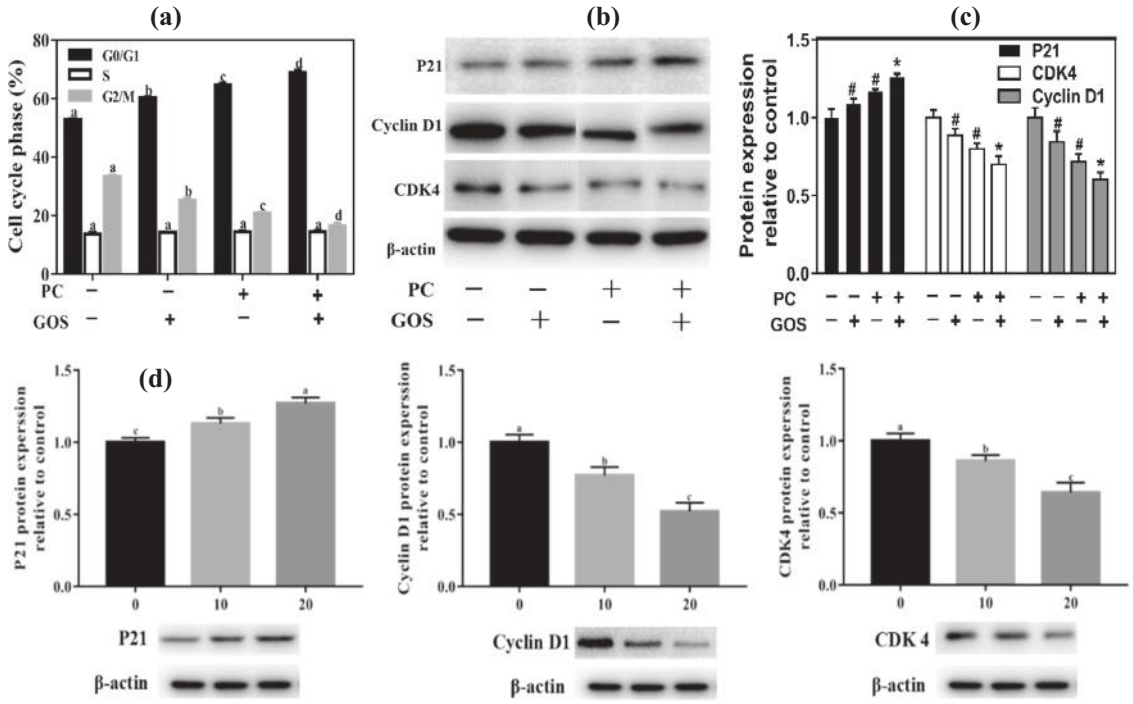

Fig. 5. (a) Effect of different sample on cell cycle distribution; (b) Western blot analysis and the percentage (c) of cell-cycle regulatory proteins in HCT116 cells after treatment with different film and (d) different concentration of PC-loaded EFM containing GOS for 48 h.

data showed that there was a significant increase in the proportion of cells induced to undergo apoptosis in PC-loaded EFM with GOS treated cells, indicating the synergistic effect by the combination of PC and GOS.

Fluorescence microscopy was also applied to characterize the morphology of apoptotic cell by PC-loaded EFM with GOS. We performed DAPI staining and PI staining assays, as shown in Fig. 6c, control cells showed homogeneous blue fluorescence and an intact nuclear structure, while the cells under the treatment of PC-loaded EFM with GOS exhibited typical characteristics of apoptosis, such as red fluorescence emission and condensed contents in the nucleolus. These observations indicated that apoptosis is one of the major mechanisms behind the anti-cancer activity of PC and GOS. Additionally, morphological analysis demonstrated that the apoptosis was enhanced by the combination treatment of PC and GOS than treatment with PC or GOS alone, suggesting that the above mentioned film-reduced cell viability was related to apoptosis. The results indicated that the combination of PC and GOS

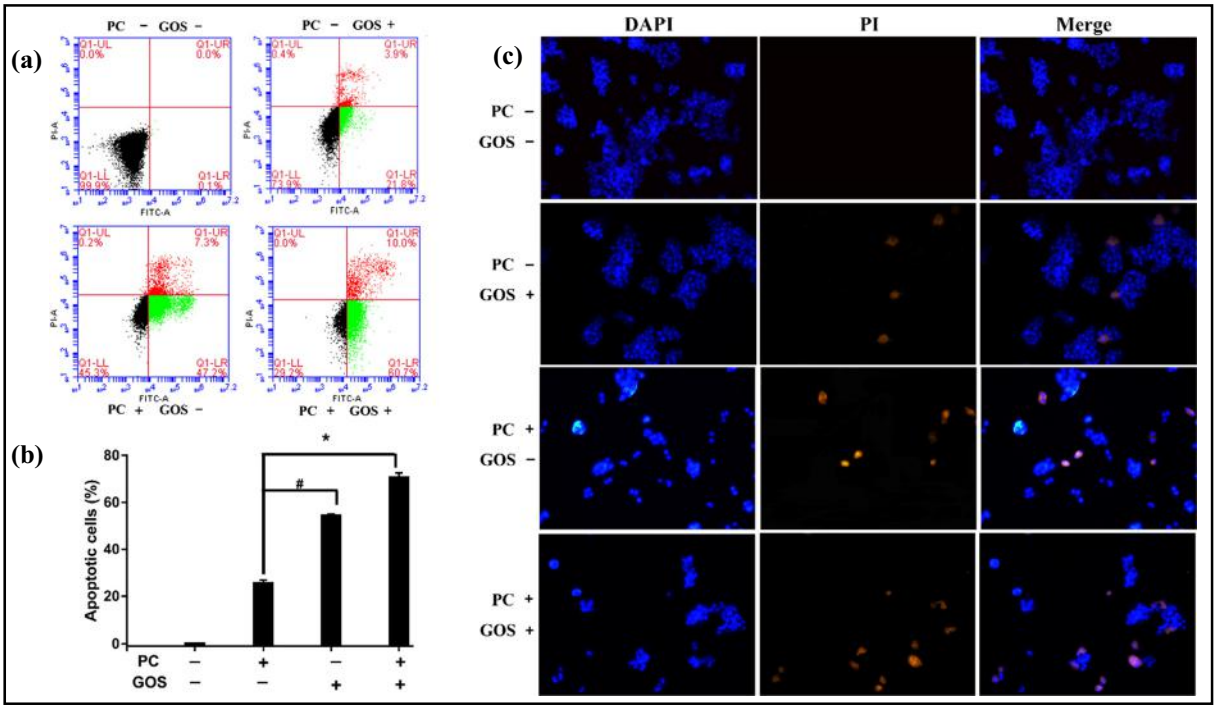

Fig. 6. (a) analysis Induction of apoptosis of HCT116 cells by Annexin V-FITC/PI double staining assay and (b) the calculated apoptosis ratio; (c) Cells were stained with DAPI and PI dye and observed using fluorescent microscopy. Healthy cells emitted blue fluorescence, and apoptotic cells emitted red fluorescence. Original magnification, ×100.

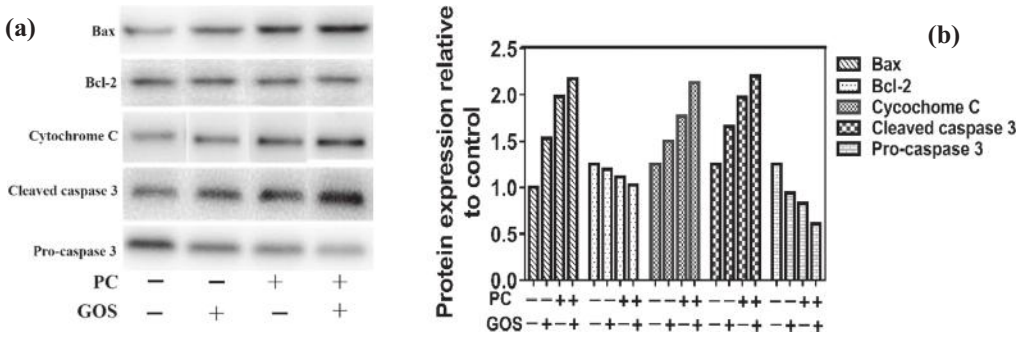

Fig. 7. (a) Western blot analysis and (b) the percentage for the relative expression of Bcl-2, Bax, Bcl-2/Bax ratio, caspase-3, C caspase-3 (cleaved caspase-3) and cytochrome C.

induced apoptosis along with the inhibition of cell cycle progression in HCT116 colon cancer cells.

Although a combination treatment of PC and GOS increased cell apoptotic activity, the action mechanism of PC-loaded EFM with GOS-induced apoptosis remains unclear. Bax and Bcl-2, the pro-apoptotic and anti-apoptotic proteins of Bcl-2 family, have been reported to be important in regulating the mitochondrial pathway of apoptosis [54]. During apoptosis, the altered ratio of Bax and Bcl-2 causes the mitochondrial potential across the membrane to collapse, leading to the release of cytochrome *c* into the cytoplasm, and thus resulting in apoptosis. Studies also showed that the Bcl gene family plays an important role in activating caspase 3 activity [55]. Given the particular importance of apoptosis regulatory proteins, herein we focused on the role of the Bcl-2 family proteins and the mitochondrial pathway in PC-loaded EFM with GOS -induced apoptosis.

As depicted in Fig. 7, an elevated level of Bax was observed, while Bcl-2 was suppressed. The data showed that exposure to PC or GOS-alone could down-regulate the ratio of Bcl-2 to Bax, which might be a cause to the accelerated apoptosis. We found that the ability to induce apoptosis in HCT 116 cells was further enhanced by co-incubation of PC and GOS, and the expression levels of tested proteins presented a dose-dependent effect treated by PC-loaded EFM with GOS. This may be because PC can improve the regulation of these apoptosis-related genes by GOS to make cells more susceptible to apoptosis. Damaged mitochondria can result in mitochondrial membrane release of several mitochondrial proteins, including cytochrome *c*, which are important for the apoptotic pathway [56]. As expected, cytochrome *c* was observed in the cytosol of PC-loaded EFM with GOS treated cells, indicating an involvement of the mitochondrial pathway in apoptosis. The translocation of cytochrome-c from the mitochondria to the cytosol results in activation of the caspase cascade and execution of apoptosis [57]. PC-loaded EFM with GOS treatment resulted in a decreased level of pro-caspase 3 and simultaneously increased the expression of the cleaved form of Caspase3. It can be concluded that Caspase3 was activated, and thus leading to apoptosis (Fig. 8). Hence, the results demonstrate apoptosis induced by PC-loaded EFM with GOS was through increase of Bax/Bcl2, activation of Caspase3 and release of cytochrome *c*.

4. Conclusions

In summary, the polysaccharides-based electrospun fiber mat (EFM) encapsulating PC and prebiotics was successfully fabricated in this

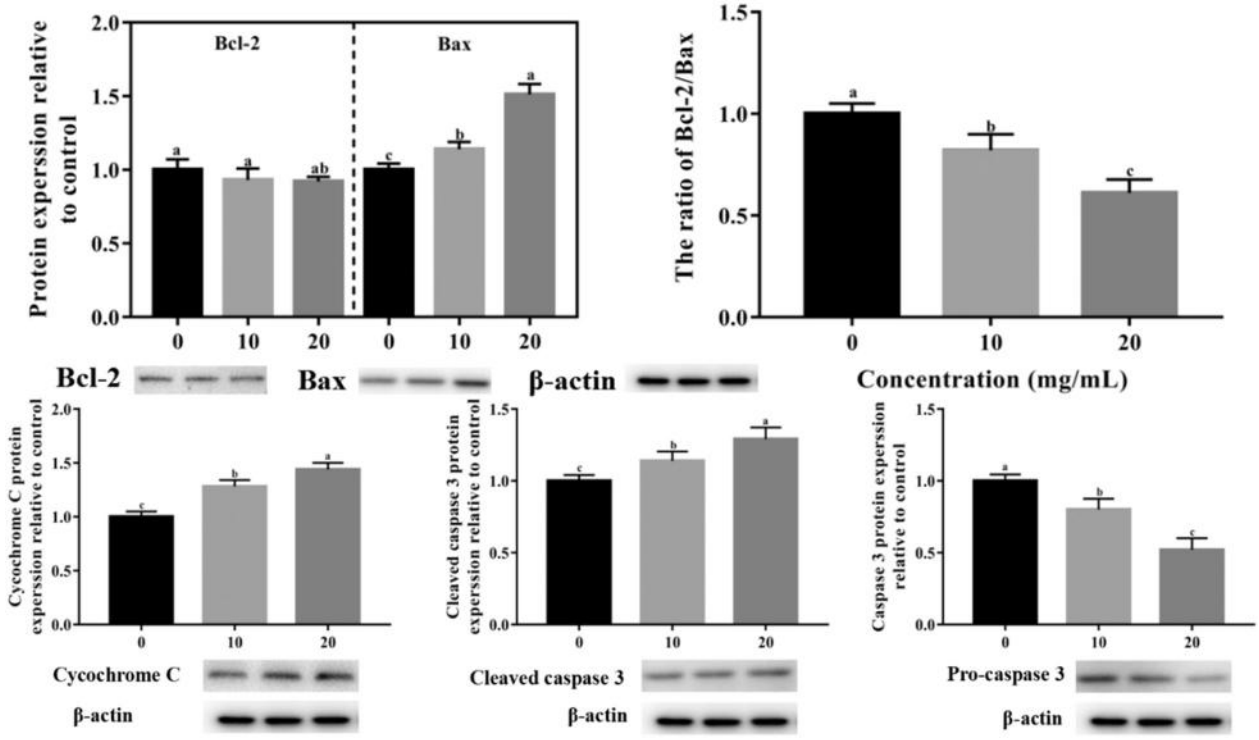

Fig. 8. Effects of different concentrations of PC-loaded EFM containing GOS on the expression levels of different proteins.

study. The presence of prebiotics leads to the enhanced colon-specific targeting property of PC, as well as the improved inhibition effect on the proliferation of human colon cancer HCT116 cells. The PC-loaded EFM with GOS synergistically blocks cell cycle and induces apoptosis in HCT116 cells. The decreased Bcl-2/Bax ratio along with the increase of cleaved caspase-3, provides evidence that the film-induced apoptosis is mediated through the mitochondrial pathway, suggesting that PC-loaded EFM with GOS is potentially a promising agent for the use in chemopreventive or therapeutics against colon cancer. Further investigation in a mouse model is necessary to explore its activity toward cancer cells in vivo.

Acknowledgments

We acknowledge the National Natural Science Foundation of China (No. 31671852), the Science and Technology Project of Guangzhou City (No. 201804010151), the National Natural Science Foundation of China (NSFC)-Guangdong Joint Foundation Key Project (No. U1501214), the Open Project Program of Provincial Key Laboratory of Green Processing Technology and Product Safety of Natural Products (KL-2018-02) and Guangdong Science and Technology Collaborative Innovation Center For Sports (2019B110210004) for financial support.

References

[1] T. Zhang, G. Zhu, B. Lu, Q. Peng, Oral nano-delivery systems for colon targeting therapy, Pharmaceutical Nanotechnology 5 (2) (2017) 83–94.
[2] S.L. Kosaraju, Colon targeted delivery systems: review of polysaccharides for encapsulation and delivery, Crit. Rev. Food Sci. Nutr. 45 (4) (2005) 251–258.
[3] N. Shah, T. Shah, A. Amin, Polysaccharides: a targeting strategy for colonic drug delivery, Expert Opinion on Drug Delivery 8 (6) (2011) 779–796.
[4] Y. Yuan, X. Xu, J. Gong, R. Mu, Y. Li, C. Wu, J. Pang, Fabrication of chitosan-coated konjac glucomannan/sodium alginate/graphene oxide microspheres with enhanced colon-targeted delivery, Int. J. Biol. Macromol. 131 (2019) 209–217.
[5] F. Heidarpour, M.R. Mohammadabadi, I.S.M. Zaidul, B. Maherani, N. Saari, A.A. Hamid, F. Abas, M.Y.A. Manap, M.R. Mozafari, Use of prebiotics in oral delivery of bioactive compounds: a nanotechnology perspective, Pharmazie 66 (5) (2011) 319–324.
[6] J. Fernández, S. Redondo-Blanco, I. Gutiérrez-del-Río, E.M. Miguélez, C.J. Villar, F. Lombó, Colon microbiota fermentation of dietary prebiotics towards short-chain fatty acids and their roles as anti-inflammatory and antitumour agents: a review, J. Funct. Foods 25 (2016) 511–522.
[7] L.Q. Jiang, Y.J. Wang, Q.F. Yin, G.X. Liu, H.H. Liu, Y.J. Huang, B. Li, Phycocyanin: a potential drug for cancer treatment, J. Cancer 8 (17) (2017) 3416–3429.
[8] K.A. Naidu, R. Sarada, G. Manoj, M.Y. Khan, M.M. Swamy, S. Viswanatha, K.N. Murthy, G.A. Ravishankar, L. Srinivas, Toxicity assessment of phycocyanin - a blue colorant from blue green alga Spirulina platensis, Food Biotechnol. 13 (1) (1999) 51–66.
[9] I.A. Siddiqui, V. Sanna, Impact of nanotechnology on the delivery of natural products for cancer prevention and therapy, Mol. Nutr. Food Res. 60 (6) (2016) 1330–1341.
[10] H. Singh, Nanotechnology applications in functional foods; opportunities and challenges, Preventive Nutrition and Food Science 21 (1) (2016) 1–8.
[11] P. Wen, M.H. Zong, R.J. Linhardt, K. Feng, H. Wu, Electrospinning: a novel nano-encapsulation approach for bioactive compounds, Trends Food Sci. Technol. 70 (2017) 56–68.
[12] Q. Xiao, L.T. Lim, Pullulan-alginate fibers produced using free surface electrospinning, Int. J. Biol. Macromol. 112 (2018) 809–817.
[13] D.G. Yu, J.J. Li, G.R. Williams, M. Zhao, Electrospun amorphous solid dispersions of poorly water-soluble drugs: a review, J. Control. Release 292 (2018) 91–110.
[14] P. Wen, D.H. Zhu, K. Feng, F.J. Liu, W.Y. Lou, N. Li, M.H. Zong, H. Wu, Fabrication of electrospun polylactic acid nanofilm incorporating cinnamon essential oil/beta-cyclodextrin inclusion complex for antimicrobial packaging, Food Chem. 196 (2016) 996–1004.
[15] M. Jin, D.G. Yu, X. Wang, C.F.G.C. Geraldes, G.R. Williams, S.W.A. Bligh, Electrospun contrast-agent-loaded fibers for colon-targeted MRI, Advanced Healthcare Materials 5 (8) (2016) 977–985.
[16] K. Wang, H.F. Wen, D.G. Yu, Y. Yang, D.F. Zhang, Electrosprayed hydrophilic nanocomposites coated with shellac for colon-specific delayed drug delivery, Mater. Des. 143 (2018) 248–255.
[17] T. Hai, X. Wan, D.G. Yu, K. Wang, Y. Yang, Z.P. Liu, Electrospun lipid-coated medicated nanocomposites for an improved drug sustained-release profile, Mater. Des. 162 (2019) 70–79.
[18] D.G. Yu, X.L. Zheng, Y. Yang, X.Y. Li, G.R. Williams, M. Zhao, Immediate release of helicid from nanoparticles produced by modified coaxial electrospraying, Appl. Surf. Sci. 473 (2019) 148–155.
[19] Q. Wang, D.G. Yu, L.L. Zhang, X.K. Liu, Y.C. Deng, M. Zhao, Electrospun hypromellose-based hydrophilic composites for rapid dissolution of poorly water-soluble drug, Carbohydr. Polym. 174 (2017) 617–625.
[20] Z.P. Liu, L.L. Zhang, Y.Y. Yang, D. Wu, G. Jiang, D.G. Yu, Preparing composite nanoparticles for immediate drug release by modifying electrohydrodynamic interfaces during electrospraying, Powder Technol. 327 (2018) 179–187.
[21] J.J. Li, Y.Y. Yang, D.G. Yu, Q. Du, X.L. Yang, Fast dissolving drug delivery membrane based on the ultra-thin shell of electrospun core-shell nanofibers, Eur. J. Pharm. Sci. 122 (2018) 195–204.
[22] Y. Xu, J.J. Li, D.G. Yu, G.R. Williams, J.H. Yang, X. Wang, Influence of the drug distribution in electrospun gliadin fibers on drug-release behavior, Eur. J. Pharm. Sci. 106 (2017) 422–430.
[23] M.A. Dehcheshmeh, M. Fathi, Production of core-shell nanofibers from zein and tragacanth for encapsulation of saffron extract, Int. J. Biol. Macromol. 122 (2019) 272–279.
[24] M. Rostami, M. Ghorbani, M. Aman Mohammadi, M. Delavar, M. Tabibiazar, S. Ramezani, Development of resveratrol loaded chitosan-gellan nanofiber as a novel gastrointestinal delivery system, Int. J. Biol. Macromol. 135 (2019) 698–705.
[25] Y.Y. Yang, Z.P. Liu, D.G. Yu, K. Wang, P. Liu, X.H. Chen, Colon-specific pulsatile drug release provided by electrospun shellac nanocoating on hydrophilic amorphous composites, Int. J. Nanomedicine 13 (2018) 2395–2404.
[26] Z. Li, H. Kang, N. Che, Z. Liu, P. Li, W. Li, C. Zhang, C. Cao, R. Liu, Y. Huang, Controlled release of liposome-encapsulated naproxen from core-sheath electrospun nanofibers, Carbohydr. Polym. 111 (2014) 18–24.
[27] L.L. Deng, Y. Li, F.Q. Feng, D. Wu, H. Zhang, Encapsulation of allopurinol by glucose cross-linked gelatin/zein nanofibers: characterization and release behavior, Food Hydrocoll. 94 (2019) 574–584.
[28] B. Ghorani, N. Tucker, Fundamentals of electrospinning as a novel delivery vehicle for bioactive compounds in food nanotechnology, Food Hydrocoll. 51 (2015) 227–240.
[29] P. Wen, T.G. Hu, Y. Wen, R.J. Linhardt, M.H. Zong, Y.X. Zou, H. Wu, Targeted delivery of phycocyanin for the prevention of colon cancer using electrospun fibers, Food Funct. 10 (2019) 1816–1825.
[30] P. Wen, M.H. Zong, T.G. Hu, L. Li, H. Wu, Preparation and characterization of electrospun colon-specific delivery system for quercetin and its antiproliferative effect on cancer cells, J. Agric. Food Chem. 66 (44) (2018) 11550–11559.
[31] R. Thangam, V. Suresh, W. Asenath Princy, M. Rajkumar, N. SenthilKumar, P. Gunasekaran, R. Rengasamy, C. Anbazhagan, K. Kaveri, S. Kannan, C-Phycocyanin from Oscillatoria tenuis exhibited an antioxidant and in vitro antiproliferative activity through induction of apoptosis and G0/G1 cell cycle arrest, Food Chem. 140 (1) (2013) 262–272.
[32] L.S. Wang, J.C. Huang, Y.L. Chen, M. Huang, G.H. Zhou, Identification and characterization of antioxidant peptides from enzymatic hydrolysates of duck meat, J. Agric. Food Chem. 63 (13) (2015) 3437–3444.
[33] P. Wen, Y. Wen, X. Huang, M.H. Zong, H. Wu, Preparation and characterization of protein-loaded electrospun fiber mat and its release kinetics, J. Agric. Food Chem. 65 (23) (2017) 4786–4796.
[34] P. Gullón, B. Gullón, A. Cardelle-Cobas, J.L. Alonso, M. Pintado, A.M. Gomes, Effects of hemicellulose-derived saccharides on behavior of lactobacilli under simulated gastrointestinal conditions, Food Res. Int. 64 (2014) 880–888.
[35] Z. Du, J. Liu, T. Zhang, Y. Yu, Y. Zhang, J. Zhai, H. Huang, S. Wei, L. Ding, B. Liu, A study on the preparation of chitosan-tripolyphosphate nanoparticles and its entrapment mechanism for egg white derived peptides, Food Chem. 286 (2019) 530–536.
[36] I. Chentir, M. Hamdi, S. Li, A. Doumandji, G. Markou, M. Nasri, Stability, biofunctionality and bio-activity of crude phycocyanin from a two-phase cultured Saharian Arthrospira sp strain, Algal Research-Biomass Biofuels and Bioproducts 35 (2018) 395–406.
[37] A.A. Kassem, S.H. Abd El-Alim, M. Basha, A. Salama, Phospholipid complex enriched micelles: a novel drug delivery approach for promoting the antidiabetic effect of repaglinide, Eur. J. Pharm. Sci. 99 (2017) 75–84.
[38] S.F. Hosseini, M.R. Soleimani, M. Nikkhah, Chitosan/sodium tripolyphosphate nanoparticles as efficient vehicles for antioxidant peptidic fraction from common kilka, Int. J. Biol. Macromol. 111 (2018) 730–737.
[39] M.P. Souza, A.F.M. Vaz, M.T.S. Correia, M.A. Cerqueira, A.A. Vicente, M.G. Carneiro-da-Cunha, Quercetin-loaded lecithin/chitosan nanoparticles for functional food applications, Food Bioprocess Technol. 7 (4) (2014) 1149–1159.
[40] X. Chen, M. Wu, Q. Yang, S. Wang, Preparation, characterization of food grade phycobiliproteins from Porphyra haitanensis and the application in liposome-meat system, Lwt-Food Science and Technology 77 (2017) 468–474.
[41] M.D. Collins, G.R. Gibson, Probiotics, prebiotics, and synbiotics: approaches for modulating the microbial ecology of the gut, Am. J. Clin. Nutr. 69 (5) (1999) 1052S–1057S.
[42] A.G.M. Leijdekkers, M. Aguirre, K. Venema, G. Bosch, H. Gruppen, H.A. Schols, In vitro fermentability of sugar beet pulp derived oligosaccharides using human and pig fecal Inocula, J. Agric. Food Chem. 62 (5) (2014) 1079–1087.
[43] A. Belenguer, S.H. Duncan, A.G. Calder, G. Holtrop, P. Louis, G.E. Lobley, H.J. Flint, Two routes of metabolic cross-feeding between Bifidobacterium adolescentis and butyrate-producing anaerobes from the human gut, Appl. Environ. Microbiol. 72 (5) (2006) 3593–3599.
[44] P.L. Ritger, N.A. Peppas, A simple equation for description of solute release II. Fickian and anomalous release from swellable devices, J. Control. Release 5 (1) (1987) 37–42.
[45] Y. Huang, H. Yu, C. Xiao, pH-sensitive cationic guar gum/poly (acrylic acid) polyelectrolyte hydrogels: swelling and in vitro drug release, Carbohydr. Polym. 69 (4) (2007) 774–783.
[46] R.F. Dorame-Miranda, D.E. Rodriguez-Felix, G.A. Lopez-Ahumada, D.D. Castro-Enriquez, J.M. Quiroz-Castillo, E. Marquez-Rios, F. Rodriguez-Felix, Effect of pH and temperature on the release kinetics of urea from wheat-gluten membranes obtained by electrospinning, Polym. Bull. 75 (11) (2018) 5305–5319.

[47] J.P. Dyer, J.M. Featherstone, L.Z. Solomon, T.J. Crook, A.J. Cooper, P.S. Malone, The effect of short-chain fatty acids butyrate, propionate, and acetate on urothelial cell kinetics in vitro: potential therapy in augmentation cystoplasty, Pediatr. Surg. Int. 21 (7) (2005) 521–526.
[48] S. Hao, Y. Yan, S. Li, L. Zhao, C. Zhang, L.Y. Liu, C.T. Wang, The in vitro anti-tumor activity of phycocyanin against non-small cell lung cancer cells, Marine Drugs 16 (6) (2018) 178–193.
[49] R. Thangam, V. Suresh, W.A. Princy, M. Rajkumar, N. SenthilKumar, P. Gunasekaran, R. Rengasamy, C. Anbazhagan, K. Kaveri, S. Kannan, C-Phycocyanin from Oscillatoria tenuis exhibited an antioxidant and in vitro antiproliferative activity through induction of apoptosis and G(0)/G(1) cell cycle arrest, Food Chem. 140 (1–2) (2013) 262–272.
[50] M. Ravi, S. Tentu, G. Baskar, S.R. Prasad, S. Raghavan, P. Jayaprakash, J. Jeyakanthan, S.K. Rayala, G. Venkatraman, Molecular mechanism of anti-cancer activity of phycocyanin in triple-negative breast cancer cells, BMC Cancer 15 (2015) 768–781.
[51] G.Y. Liao, B. Gao, Y.N. Gao, X.G. Yang, X.D. Cheng, Y. Ou, Phycocyanin inhibits tumorigenic potential of pancreatic cancer cells: role of apoptosis and autophagy, Sci. Rep. 6 (2016) 34564–34576.
[52] A. Lan, D. Lagadic-Gossmann, C. Lemaire, C. Brenner, G. Jan, Acidic extracellular pH shifts colorectal cancer cell death from apoptosis to necrosis upon exposure to propionate and acetate, major end-products of the human probiotic propionibacteria, Apoptosis 12 (3) (2007) 573–591.
[53] S. Rao, M. Lowe, T.W. Herliczek, K. Keyomarsi, Lovastatin mediated G1 arrest in normal and tumor breast cells is through inhibition of CDK2 activity and redistribution of p21 and p27, independent of p53, Oncogene 17 (18) (1998) 2393–2402.
[54] L. Leanza, B. Henry, N. Sassi, M. Zoratti, K.G. Chandy, E. Gulbins, I. Szabò, Inhibitors of mitochondrial Kv1.3 channels induce Bax/Bak-independent death of cancer cells, EMBO Molecular Medicine 4 (7) (2012) 577–593.
[55] J. Zhou, S. Zhang, O. Choon-Nam, H.-M. Shen, Critical role of pro-apoptotic Bcl-2 family members in andrographolide-induced apoptosis in human cancer cells, Biochem. Pharmacol. 72 (2) (2006) 132–144.
[56] L. Galluzzi, O. Kepp, C. Trojel-Hansen, G. Kroemer, Mitochondrial control of cellular life, stress, and death, Circ. Res. 111 (9) (2012) 1198–1207.
[57] F.M. Ruemmele, S. Schwartz, E.G. Seidman, S. Dionne, E. Levy, M.J. Lentze, Butyrate induced Caco-2 cell apoptosis is mediated via the mitochondrial pathway, Gut 52 (1) (2003) 94–100.